———., and C. J. King, "Losses of Volatiles in the Nozzle Zone During Spray Drying," paper presented at the Second Pacific Chemical Engineering Congress, Denver, Colo. (1977).
———., "An Improved Method of Determining Vapor-Liquid Equilibria for Dilute Organics in Aqueous Solution," *J. Chromatog. Sci.*, **17**, 273 (1979*a*).
———., "Partition Coefficients for Acetates in Food Systems," *J. Agr. Food Chem.*, **27**, 504 (1979*b*).
Lapple, C. E., J. P. Henry and D. E. Blake, "Atomization—A Survey and Critique of the Literature," *S. R. I. Tech. Rept. No. 6*, Stanford Res. Inst., Stanford, Ca. (1967).
Lin, W-C., P. A. Rice, Y-S. Cheng and A. J. Barduhn, "Vacuum Stripping of Refrigerants in Water Sprays," *AIChE J.*, **23**, 409 (1977).
Reineccius, G. A., and S. T. Coulter, "Flavor Retention During Drying," *J. Dairy Sci.*, **52**, 1219 (1969).
Rothe, P. H., and J. A. Block, "Aerodynamic Behavior of Liquid Sprays," *Int. J. Multi-phase Flow*, **3**, 263 (1977).
Rulkens, W. H., "Retention of Volatile Trace Components in Drying Aqueous Carbohydrate Solutions," Ph.D. dissertation, Eindhoven Univ. of Technology, Holland (1973).
———., and H. A. C. Thijssen, "The Retention of Organic Volatiles in Spray Drying Aqueous Carbohydrate Solutions," *J. Food Technol.*, **7**, 95 (1972).
Sherwood, T. K., R. L. Pigford and C. R. Wilke, *Mass Transfer*, p. 80, McGraw-Hill, New York (1977).
Simpson, S. G., "Vacuum Stripping of Sparingly Soluble Gases from H_2O," Ph.D. dissertation, Univ. Calif., Berkeley (1975).
———., and S. Lynn, "Vacuum-Spray Stripping of Sparingly Soluble Gases from Aqueous Solutions," *AIChE J.*, **23**, 666 (1977).
Thijssen, H. A. C., and W. H. Rulkens, "Retention of Aromas in Drying Food Liquids," *De Ingenieur* (The Hague), Vol. 80, Ch 45 (1968).

Manuscript received August 4, 1978; revision received July 23, and accepted August 30, 1979.

Multiplicity and Stability of the Hydrogen-Oxygen-Nitrogen Flame: The Influence of Chemical Pathways and Kinetics on Transitions Between Steady States

ROBERT F. HEINEMANN
KNOWLES A. OVERHOLSER
and
GEORGE W. REDDIEN

Departments of Chemical Engineering and Mathematics
Vanderbilt University
Nashville, Tennessee 37235

Numerical bifurcation techniques are used to predict multiple steady states for a nonadiabatic, premixed hydrogen flame stabilized on a flat-flame burner. It is found that predicted conditions for burnout and ignition vary remarkably as rival chemical models are selected, while conditions for a well-stabilized flame are much less sensitive to chemical and kinetic assumptions. It is concluded that multiplicity theory can help define the chemical behavior of realistic, complex reaction-diffusion systems.

SCOPE

The use of theoretical predictions of multiplicity in the identification of kinetic parameters of combustion systems has been proposed by several workers (Smith et al., 1971; Fang et al., 1971; Williams, 1971; Berlad, 1973; Heinemann et al., 1979). Such an approach may be particularly useful for flames in which transitions between steady states correspond to the readily identifiable phenomena of burnout and ignition. We (Heinemann et al., 1979) have previously applied numerical bifurcation techniques (Keller, 1977) to a simple A → products flame and have shown that the solutions are particularly sensitive to changes in reaction rate coefficients near burnout.

In the present work, we apply such methods to the nonadiabatic, premixed, hydrogen flame stabilized on a flat-flame burner. Although the chemical mechanism of this flame is complex enough to afford a practical test of the use of multiplicity theory in discriminating between rival chemical pathways, the individual steps are well understood (Dixon-Lewis, 1970). Two mechanisms are studied: a seven-step mechanism involving hydroperoxyl radicals and a simple, four-step subset of the more complete model.

Correspondence concerning this paper should be addressed to K. A. Overholser. R. F. Heinemann is with the Chemical Engineering Department and the Mathematics Research Center, The University of Wisconsin, Madison, Wisconsin, 53705. G. W. Reddien is with the Department of Mathematics, Southern Methodist University, Dallas, Texas, 75275.

0001-1541-80-3623-0725-$01.15.

CONCLUSIONS AND SIGNIFICANCE

For both the simple and hydroperoxyl mechanisms, three steady state solutions were obtained over a wide range of burner temperatures. High temperature solutions correspond to stable, nonadiabatic flames. As the burner temperature is lowered, the flames lose less heat to the burner surface, eventually approaching adiabaticity and burnout. This sequence of events corresponds to transition to another stable mathematical solution, the low temperature, extinguished state. Between the upper and lower solutions lies an unstable, intermediate state.

Although for well-stabilized, nonadiabatic flames, predictions of temperature and concentration profiles differ but little between the two rival mechanisms, predicted temperatures at burnout and ignition are highly sensitive to choice of chemical model. For example, the simple mechanism predicts an unreasonably low ignition temperature of 580°K, while the seven-step model predicts ignition at 860°K. Such differences can be explained by a comparison of the details of the two mechanisms. The seven-step model includes hydroperoxyl pathways, wherein hydrogen radicals are rapidly consumed. Autothermal ignition, which relies on the availability of radicals, is postponed until burner temperature is high. The failure of the simpler model to include provision for effective depletion of hydrogen radicals at low temperatures accounts for the unrealistic ignition temperature predicted by the four-step scheme.

Within the seven-step model, sensitivity of predicted behavior to changes in reaction rate coefficients is enhanced near transition points. The effect of the rate coefficient of a hydrogen radical recombination step on heat release and on hydrogen concentration explains shifts in the location of burnout and ignition.

We conclude that numerical descriptions of reacting systems near transitions may be useful in discriminating between rival chemical models and in measuring reaction rate coefficients. Furthermore, examination of changes in temperature and concentration profiles near transitions contributes to our understanding of chemical events associated with ignition and extinction.

There are several reasons for examining multiplicity and stability of reacting systems. From one point of view, one might hope to control an industrial reactor to operate in the most economical of several potentially accessible steady states. Alternately, the designer might use theory to avoid operating near transitions to undesirable or dangerous steady states or limit cycles. A third justification of the effort and expense involved in the investigation of multiplicity is the possibility of comparing theoretical and experimental behavior of uncontrolled systems near instability in order to learn more about the chemistry of complex reactions. This point of view, emphasized in the present work, assumes that near transitions between steady states predicted behavior may be particularly sensitive to changes in assumed parameters such as reaction rate coefficients. Furthermore, the conditions under which transitions between steady states are predicted might be changed substantially as one makes various assumptions about the existence or importance of competing chemical pathways. Agreement between theory and experiment might be altered decisively as rival models are tested. Thus, theoretical studies of multiplicity and stability may be viewed as aids to the understanding of chemistry and kinetics.

Whatever the motivation, the continuous, stirred-tank reactor (CSTR) has received a great deal of attention over the past decade. Poore (1973) and Uppal et al. (1974, 1976) present an important and thorough consideration of the single, first-order exothermic reaction in the CSTR. More recently, Chang and Calo (1979) use the implicit function theorem to derive exact bounds of multiplicity for an n^{th} order reaction in an adiabatic or nonadiabatic CSTR. There are appropriate reasons for concentrating attention on the CSTR (Schmitz, 1975): the mathematics are comparatively tractable, studies of the CTSR help in the understanding of more complex reactors and the CSTR is a limiting case of the tubular flow reactor (Cohen and Poore, 1974). Nevertheless, in some ways it is advantageous to study reactors in which the mathematical model must predict spatial as well as temporal variations of temperature and concentration. One such distributed parameter system, the tubular flow reactor, has been studied in detail for simple reactions (see, for example, Varma and Amundson, 1972*a*, *b*, 1973*a*, *b*). Distributed parameter systems are particularly interesting if one is concerned with using theoretical predictions to help determine reaction rate coefficients, for the requirement that the kinetic model predict concentration and temperature profiles as well as transitions between steady states imposes additional constraints upon the kinetic parameters.

Viewed as a special case of the tubular reactor, the premixed flame is an attractive subject for the theoretical investigation of multiplicity. Flames are highly exothermic and usually involve autocatalytic or autothermal reaction chains, features associated with the presence of multiple steady states. (Flames certainly exhibit at least two steady states. Transitions between the two are called burnout and ignition.) Furthermore, the transport phenomenological aspects of modeling the laminar, premixed flame are relatively straightforward compared, say, to the uncertainties associated with the description of the heterogenous, catalytic, tubular reactor. Since one can have more confidence in the ability of the model to accurately describe the physics of the flame, one can more assuredly use the model to study chemical features.

Few studies of multiple steady states in open combustion systems are to be found in the literature. Schmitz and coworkers have identified multiple steady states for a planar diffusion flame (Kirkby and Schmitz, 1966; Schmitz, 1967) and for a premixed combustion system in adiabatic stagnation flow (Smith et al., 1971; Fang et al., 1971). Both studies revealed the existence of three steady states: the stable ignited state, a stable extinguished state and an unstable intermediate solution. In the case of the stagnation flow system, the possibility of distinguishing between rival kinetic schemes for the oxidation of carbon monoxide by comparing theory and experiment near the quench point was proposed.

For the simple A → products reaction, analytical solutions of the flame equations have been obtained in the limit of large activation energy by Carrier et al. (1978). In this limit, for which the reaction zone approaches infinitesimal thickness, Carrier et al. found that the heat transfer for the burner is a unique function of flow rate.

We (Heinemann et al., 1979) have applied numerical bifurcation techniques to a mathematical model of a premixed, laminar flame stabilized on a flat-flame burner. The flame was assumed to be adiabatic, and the kinetic mechanism was approximated by a single A → B reaction. For realistic choices of the frequency factor, activation energy and exothermicity, the flame exhibited

three steady states, one of which was unstable. Transition from the stable burning state to extinction was quite sensitive to reaction order and to changes in kinetic parameters, even though temperatures in a well-stabilized flame were insensitive to similar changes.

It was the goal of the present work to extend such methodology to the nonadiabatic hydrogen flame. This system was chosen because the steps in the chain reaction are relatively well understood. It was our opinion that the hydrogen flame could serve as an example of the use of the theory of multiplicity and stability to help explore details of an important, complex and realistic reaction scheme.

REACTION KINETICS OF THE HYDROGEN-OXYGEN-NITROGEN FLAME

The kinetic mechanism describing the hydrogen-oxygen-nitrogen flame has been studied extensively by Dixon-Lewis and co-workers (1967, 1970, 1972, 1975). The complete mechanism consists of at least twelve reactions. The flame studied in the present work is rich in hydrogen (18.8 mole % hydrogen, 17.6% nitrogen, 4.6% oxygen at the inlet), and at such concentrations one is justified in neglecting several reaction steps contained in the complete mechanism.

The simplest mechanism which adequately describes the kinetics of the rich hydrogen-oxygen-nitrogen flame is shown below:

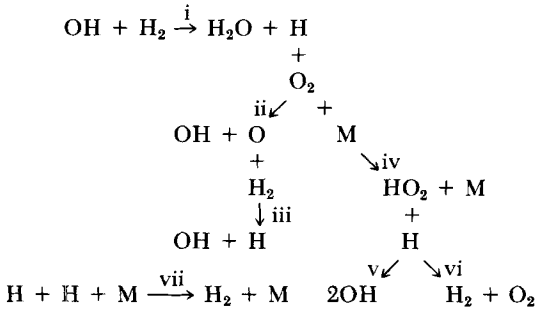

The third body M in reactions (iv) and (vii) represents any stable species in the mechanism and removes the energy released when the water and hydrogen chemical bonds are formed. This energy must be removed by a collision with the third body within a few vibrational periods of the molecules or they will redissociate. The required time is so short that the third body collision is nearly simultaneous with the collision of the two reactants. Hence, the reaction process is effectively trimolecular (Fristrom and Westenberg, 1965).

In the oxygen deficient flame, the steps consuming oxygen molecules are assumed to be rate controlling. Furthermore, hydroxyl and oxygen radicals formed in reactions (ii), (iii) and (v) react immediately in steps (i) and (iii), while the hydroperoxyl radicals produced in (iv) are immediately consumed by (v) and (vi).

The above assumptions allow the original mechanism of seven reaction steps and six reactants to be condensed to a four-step mechanism with only two reactants, hydrogen atoms and oxygen molecules, whose concentrations are independent. The first three reactions of the original mechanism can be combined to give a hydrogen radical initiation step:

$$H + O_2(+3H_2) \rightarrow 2H_2O + 3H \qquad \text{(ii-}a\text{)}$$

(The species in parentheses are included to balance the stoichiometry of the reaction and do not influence the reaction rate.) Reactions (iv), (v) and (i) can be combined to yield a chain propagation reaction:

$$H + O_2 + M(+H + 2H_2) \rightarrow 2H_2O + 2H + M \qquad \text{(iv-}a\text{)}$$

A hydrogen radical termination step is formed from reaction (iv) and (vi):

$$H + O_2 + M(+H) \rightarrow H_2 + O_2 + M \qquad \text{(iv-}b\text{)}$$

Reaction (vii) is also a radical recombination reaction and cannot be combined with any other step.

Dixon-Lewis (1970) reports that the reaction rates of the four-step mechanism are controlled by the rate constants k_2, k_4, k_7 and the ratio k_5/k_6. Reaction rate expressions for the five species contained in the complete mechanism are

$$r_{OH} = -k_1 C_{OH} C_{H_2} + k_2 C_H C_{O_2} + k_3 C_O C_{H_2} + 2k_1 C_H C_{HO_2} \qquad (1)$$

$$r_O = k_2 C_H C_{O_2} - k_3 C_O C_{H_2} \qquad (2)$$

$$r_{HO_2} = k_4 C_H C_{O_2} C_M - k_5 C_{HO_2} C_H - k_6 C_H C_{HO_2} \qquad (3)$$

$$r_{O_2} = -k_2 C_H C_{O_2} - k_4 C_H C_{O_2} C_M + k_6 C_H C_{HO_2} \qquad (4)$$

$$r_H = k_1 C_{OH} C_{H_2} - k_2 C_H C_{O_2} + k_3 C_O C_{H_2} - k_4 C_H C_{O_2} C_M - k_5 C_H C_{OH_2} - k_6 C_H C_{HO_2} - 2k_7 C_H^2 C_M \qquad (5)$$

The application of the steady state assumption to the hydroxyl, oxygen and hydroperoxyl radicals gives

$$C_{OH} = \frac{2k_2 C_H C_{O_2} + \dfrac{2(k_5/k_6)k_4}{1 + (k_5/k_6)} C_H C_{O_2} C_M}{k_1 C_{H_2}} \qquad (6)$$

$$C_O = \frac{k_2 C_H C_{O_2}}{k_3 C_{H_2}} \qquad (7)$$

$$C_{HO_2} = \frac{k_4}{k_5 + k_6} C_{O_2} C_M \qquad (8)$$

Substitution of these concentrations in Equations (4) and (5) yields

$$r_{O_2} = -k_2 C_H C_{O_2} - \frac{(k_5/k_6)k_4}{1 + (k_5/k_6)} C_H C_{O_2} C_M \qquad (9)$$

$$r_H = 2k_2 C_H C_{O_2} - \frac{2k_4}{1 + (k_5/k_6)} C_H C_{O_2} C_M - 2k_7 C_H^2 C_M \qquad (10)$$

Inspection of (9) and (10) reveals that k_2 is the appropriate rate constant for reaction (ii-a); the rate constants for the chain propagation reaction (iv-a) and the termination reaction (iv-b) are

$$k_p = \frac{(k_5/k_6)k_4}{1 + (k_5/k_6)} \qquad k_t = \frac{k_4}{1 + (k_5/k_6)} \qquad (11)$$

The Arrhenius expressions suggested by Dixon-Lewis (1970) for k_2, k_4, k_7 and (k_5/k_6) are presented in Table 1 along with the appropriate heats of reaction.

TABLE 1. REACTION RATE CONSTANTS AND HEATS OF REACTION

$k_2 = 2.05 \times 10^{11} \exp(-E_2/RT)$ m³/(mole · s)

$E_2 = 6.908 \times 10^7$ J/mole

$k_{4,H_2} = \begin{cases} 4.505 \times 10^{12} \exp(-E_4/RT) \text{ m}^6/(\text{mole}^2 \cdot \text{s}) & \text{(hydroperoxyl)} \\ 0 & \text{(simple)} \end{cases}$

$E_4 = -6.280 \times 10^6$ J/mole

$k_5/k_6 = 5 \pm 1$

$k_{7,N_2} = k_{7,O_2} = k_{7,H_2O} = \begin{cases} 4.50 \times 10^9 \text{m}^6/(\text{mole}^2 \cdot \text{s}) & \text{(hydroperoxyl)} \\ 8.35 \times 10^8 \text{m}^6/(\text{mole}^2 \cdot \text{s}) & \text{(simple)} \end{cases}$

$k_{7,H_2} = 6.5\, k_{7,N_2}$

$\Delta H = 4.773 \times 10^7$ J/mole

$\Delta H_p = 4.840 \times 10^8$ J/mole

$\Delta H_t = 4.363 \times 10^8$ J/mole

$\Delta H_7 = 4.363 \times 10^8$ J/mole

The kinetics of the rich hydrogen-oxygen-nitrogen flame can be approximated by mechanisms simpler than the one presented above. Dixon-Lewis (1967) has employed a mechanism consisting of hydrogen atoms and oxygen molecules. The suggested rate constants for the simple mechanism are presented in Table 1. Dixon-Lewis found this model to predict reasonable temperature and oxygen profiles, but the atomic hydrogen concentrations are extremely high. This result, coupled with experimental evidence which indicated that the reactions involving hydroperoxyl radicals are faster than (ii), led to the inclusion of reactions (iv), (v) and (vi) in the kinetic mechanism. The effect of the simple, two-step mechanism on flame multiplicity and temperature and concentration profiles are compared with the predictions of the more complex mechanism in a later section of this work.

THE MATHEMATICAL MODEL OF THE HYDROGEN-OXYGEN-NITROGEN FLAME

The mathematical model describes a one-dimensional, premixed, hydrogen-oxygen-nitrogen flame stabilized on a cooled, flat-flame burner. The following assumptions are used to simplify the conservation equations:

1. The flow is laminar, and the velocity profile is flat.
2. Pressure is constant.
3. Radiation is negligible.
4. Viscous and body forces are unimportant.
5. The gases are ideal.
6. A pseudobinary Fick's law governs the diffusion of each species with respect to the total mixture.
7. Soret and Dufour effects are negligible.
8. The specific heats of all species are constant and equal.
9. The product $\rho^2 D$ is constant for all species. In addition, $\rho^2 D_{O_2} = \rho k/C_p$, implying that the Lewis number based on D_{O_2} is unity.

The above assumptions are common in flame modeling. The first assumption arises from the fluid dynamics of the flat-flame burner. The burner head contains numerous, minute holes emitting individual Poiseuille velocity profiles of gas which merge into a single flat velocity profile. Pressure is constant since the gas velocities through the entire flame are much less than the speed of sound. Fristrom and Westenberg (1965) use a macroscopic momentum balance to show the change in pressure through flat flames is less than 10^{-6} atm.

Radiation in the rich hydrogen flame is unimportant, since the concentrations of heteronuclear molecules, which emit thermal radiation, and excited radicals, which emit chemiluminescent radiation, are extremely low (Fristrom and Westenberg, 1965).

The neglect of viscous and body forces is consistent with assumption (2) and eliminates the equation of motion from the mathematical flame model. Assumption (5) is valid for the relatively low pressures and temperatures of the rich hydrogen flame (Fristrom and Westenberg, 1965). The pseudobinary Fick's law, employed in the species continuity equations, accurately approximates the multicomponent diffusion occurring in the flame since molecular oxygen and atomic hydrogen are present in small amounts (Dixon-Lewis, 1970).

Assumption (7) results from experimental observations of flame behavior (Kanury, 1975; Fristrom and Westenberg, 1965). Assumptions (8) and (9) are not essential to the analysis of the hydrogen flame and are chosen for computational reasons. The assumptions allow the analysis of model under the approximation of constant $\rho^2 D$ and $\rho k/C_p$ and facilitate comparison to earlier studies (Margolis, 1978).

Under these assumptions, the equation expressing the conservation of oxygen molecules becomes

$$\rho\frac{\partial \omega_{O_2}}{\partial t} + \rho v\frac{\partial \omega_{O_2}}{\partial x} = \frac{\partial}{\partial x}\rho D_{O_2}\frac{\partial \omega_{O_2}}{\partial x} - \frac{A_2\rho^2\omega_{O_2}\omega_H}{MW_H}\exp(-E_2/RT) - \frac{A_p\rho^3\omega_H\omega_{O_2}\omega_M}{MW_H MW_M}\exp(-E_p/RT) \quad (12)$$

Similarly, the continuity equation for hydrogen atoms is

$$\rho\frac{\partial \omega_H}{\partial t} + \rho v\frac{\partial \omega_H}{\partial x} = \frac{\partial}{\partial x}\rho D_H\frac{\partial \omega_H}{\partial x} + \frac{2A_2\rho^2\omega_{O_2}\omega_H}{MW_{O_2}}\exp(-E_2/RT) - \frac{2A_t\rho^3\omega_H\omega_{O_2}\omega_M}{MW_{O_2}MW_M}\exp(-E_t/RT) - \frac{2A_7\rho^3\omega_H^2\omega_M}{MW_M MW_H} \quad (13)$$

The energy equation is

$$\rho C_p\frac{\partial T}{\partial t} + \rho v\, C_p\frac{\partial T}{\partial x} = \frac{\partial}{\partial x}k\frac{\partial T}{\partial x} + \frac{\Delta H_2 A_2\rho^2\omega_{O_2}\omega_H}{MW_{O_2}MW_H}\exp(-E_2/RT) + \frac{\Delta H_p A_p\rho^3\omega_H\omega_{O_2}\omega_M}{MW_H MW_{O_2}MW_M}\exp(-E_p/RT) + \frac{\Delta H_t A_t\rho^3\omega_H\omega_{O_2}\omega_M}{MW_H MW_{O_2}MW_M}\exp(-E_t/RT) + \frac{\Delta H_7 A_7\rho^3\omega_H^2\omega_M}{MW_M MW_H^2} \quad (14)$$

Equations (12) to (14) may be cast in simpler form by change of variable:

$$d\psi = \rho dx \quad (15)$$

Furthermore, the equations may be nondimensionalized using the following definitions:

$$y = \frac{\omega_{O_2}}{\omega_{O_2C}} \qquad z = \frac{\omega_H}{\omega_{O_2C}}$$

$$u = \frac{\omega_M}{\omega_{O_2C}} \qquad \theta = \frac{T}{T_C}$$

$$s = \frac{\psi - \psi_C}{\psi_H - \psi_C} \qquad Pe_T = \frac{\rho v(\psi_H - \psi_C)}{\rho k/C_p}$$

$$Pe_O = \frac{\rho v(\psi_H - \psi_C)}{\rho^2 D_{O_2}} \qquad Pe_H = \frac{\rho v(\psi_H - \psi_C)}{\rho^2 D_H}$$

$$\Lambda_2 = \frac{A_2\rho_C\omega_{O_2C}(\psi_H - \psi_C)^2}{MW_{O_2}\rho^2 D_{O_2}} \qquad \Lambda_p = \frac{A_p\rho_C^2\omega_{O_2C}^2(\psi_H - \psi_C)^2}{MW_{O_2}MW_M\rho^2 D_{O_2}}$$

$$\Lambda_t = \frac{A_t\rho_C^2\omega_{O_2C}^2(\psi_H - \psi_C)^2}{MW_{O_2}MW_M\rho^2 D_{O_2}} \qquad \Lambda_7 = \frac{A_7\rho_C^2\omega_{O_2C}^2(\psi_H - \psi_C)^2}{MW_M MW_H\rho^2 D_{O_2}}$$

$$B_2 = \frac{\Delta H_2\omega_{O_2C}}{C_p T_C MW_H} \qquad B_p = \frac{\Delta H_p\omega_{O_2C}}{C_p T_C MW_H}$$

$$B_t = \frac{\Delta H_t\omega_{O_2C}}{C_p T_C MW_H} \qquad B_7 = \frac{\Delta H_7\omega_{O_2C}}{C_p T_C MW_H}$$

$$\gamma_2 = \frac{E_2}{RT_C} \qquad \gamma_p = \frac{E_p}{RT_C}$$

$$\gamma_t = \frac{E_t}{RT_C} \qquad R_1 = \frac{MW_{O_2}}{MW_H}$$

$$R_2 = \frac{\rho^2 D_{O_2}}{\rho^2 D_H}$$

For the steady state conditions, the resulting equations are

$$\frac{d^2y}{ds^2} - Pe_O\frac{dy}{ds} - R_1\left(\frac{2\Lambda_2 yz}{\theta}\exp(-\gamma_2/\theta) + \frac{\Lambda_p yzu}{\theta^2}\exp(-\gamma_p/\theta)\right) = 0 \quad (16)$$

$$\frac{d^2z}{ds^2} - Pe_H \frac{dz}{ds} + R_2\left(\frac{2\Lambda_2 yz}{\theta}\exp(-\gamma_2/\theta) - \frac{2\Lambda_t yzu}{\theta^2}\exp(-\gamma_t/\theta) - \frac{2\Lambda_7 z^2 u}{\theta^2}\right) = 0 \quad (17)$$

$$\frac{d^2\theta}{ds^2} - Pe_T \frac{d\theta}{ds} + \frac{B_2\Lambda_2 yz}{\theta}\exp(-\gamma_2/\theta) + \frac{B_p\Lambda_p yzu}{\theta^2}\exp(-\gamma_p/\theta) + \frac{B_t\Lambda_t yzu}{\theta^2}\exp(-\gamma_t/\theta) + \frac{B_7\Lambda_7 z^2 u}{\theta^2} = 0 \quad (18)$$

At the cold boundary of the flame, the temperature of the reactants is presumed to be fixed and equal to the temperature of the burner surface. The boundary conditions for hydrogen and oxygen are derived from material balances written about the flame entrance under the assumption of no chemical reaction at the entrance. These conditions, discussed in greater detail by Spalding and Stephenson (1971), Margolis (1978) and Bischoff (1961), are written below:

$$\text{at } s = 0 \qquad \frac{dy}{ds} = Pe_O(y - 1)$$

$$\frac{dz}{ds} = Pe_H z$$

$$\theta = 1 \quad (19)$$

At the hot boundary, temperature and concentration profiles are assumed to be flat:

$$\text{at } s = 1 \qquad \frac{dy}{ds} = \frac{dz}{ds} = \frac{d\theta}{ds} = 0 \quad (20)$$

The above model uses the more complete hydroperoxyl mechanism for the kinetic description of the rich hydrogen flame. The mathematical model of the flame for the simpler, two-step kinetic mechanism consists of Equations (16) through (20) with $\Lambda_p = \Lambda_t = 0$.

The physical and chemical parameters shown in Table 2 were used in our theoretical analysis of the rich hydrogen-oxygen-nitrogen flame and were derived from the works of Dixon-Lewis et al. (1967, 1970). The value of ρv was selected to correspond to an inlet velocity of 0.132 m/s at a density of 0.589 kg/m^3. The model parameters, computed from the kinetic and thermodynamic constants shown in Table 1, appear in Table 3. The cold boundary temperature T_C is removed from the dimensionless parameters, since T_C was chosen as the eigenvalue of the problem.

When centered difference approximations are used to discretize the derivatives in Equations (16) to (20), numerical bifurcation techniques can be applied to the flame model. These techniques are discussed in the next section.

Table 2. Physical and Chemical Parameters of the Rich Hydrogen-Oxygen-Nitrogen Flame

$\rho v = 7.77 \times 10^{-2}$ kg/(m^2 · s)

$\omega_{O_2 C} = 0.063$

$\rho^2 D_{O_2} = 2.37 \times 10^{-5}$ kg^2/(m^4 · s)

$\rho^2 D_H = 13.4 \times 10^{-5}$ kg^2/(m^4 · s)

$C_p = 1.292 \times 10^3$ J/(kg · K)

$\psi_H - \psi_C = 3.9 \times 10^{-3}$ kg/m^2

NUMERICAL METHODS

We expect the model of the hydrogen flame to exhibit multiple solutions. If so, transitions between steady states will occur at limit points or bifurcation points. Severe computational difficulties are encountered near such singularities. Numerical methods due to Keller (1977) compute entire steady state solution branches, skip over singular points and compute all solutions intersecting at a bifurcation point.

These techniques have been successfully applied to a mathematical model of the single-reaction, adiabatic flat flame (Heinemann et al., 1979) and are preferred over numerical methods used in earlier multiplicity studies. The methods are quite efficient and can be directly applied to homogeneous and heterogeneous chemical reactors and to other complex reaction-diffusion systems.

Equations (16) to (20) can be written in the form

$$G(u, \lambda) = 0 \quad (21)$$

where u represents the steady state solutions and λ is an independently chosen parameter (in our case, the cold boundary temperature). The Euler-Newton continuation method can be used to solve problem (21), with Euler's method (22) serving as a predictor for Newton's method (23):

$$u^0(\lambda - \delta\lambda) = u(\lambda) + \delta\lambda \frac{du(\lambda)}{d\lambda} \quad (22)$$

$$u^{\nu+1}(\lambda + \delta\lambda) = u^\nu(\lambda + \delta\lambda) - G_u^{-1}(u^\nu(\lambda + \delta\lambda), \lambda + \delta\lambda)\, G(u^\nu(\lambda + \delta\lambda), \lambda + \delta\lambda) \quad (23)$$

However, this technique fails near limit or bifurcation points, since the Jacobian matrix G_u cannot be inverted near singularities.

Keller (1977) has shown that by imposing an additional normalization on the solution, entire branches can be traced, skipping over singular points. The imposition of this normalization allows the specification of a new parameter s which replaces λ as the continuation parameter in the Euler-Newton technique. The reparameterized problem becomes

$$P(x, s) = 0 \quad (24)$$

where

Table 3. Parameters Used in the Mathematical Model of the Rich Hydrogen-Oxygen-Nitrogen Flame

$Pe_O = Pe_T = 12.78$

$Pe_H = 2.26$

$\Lambda_2 T_C = 7.37 \times 10^{10}$K

$\Lambda_p T_C{}^2 = \begin{cases} 1.04 \times 10^9 K^2 \text{ (hydroperoxyl)} \\ 0 \text{ (simple)} \end{cases}$

$\Lambda_t T_C{}^2 = \begin{cases} 2.08 \times 10^8 K^2 \text{ (hydroperoxyl)} \\ 0 \text{ (simple)} \end{cases}$

$\Lambda_7 T_C{}^2 = \begin{cases} 3.99 \times 10^{10} K^2 \text{ (hydroperoxyl)} \\ 0 \text{ (simple)} \end{cases}$

$B_2 T_C = 2\,335.8$°K

$B_p T_C = 23\,685.8$°K

$B_t T_C = 21\,350.0$°K

$B_7 T_C = 21\,350.0$°K

$\gamma_2 T_C = 8\,250.0$°K

$\gamma_p T_C = \gamma_t T_C = -750.0$°K

$$x(s) = [u(s), \lambda(s)] \tag{25}$$

and

$$P[x(s), s] = \begin{pmatrix} G[u(s), \lambda(s)] \\ N[u(s), \lambda(s), s] \end{pmatrix} \tag{26}$$

We have chosen the normalization $N(u,\lambda,s)$ such that s approximates the arc length of the solution branch for some parameter:

$$N_2(u,\lambda,s) = \alpha\|u(s) - u(s_0)\|^2 + (1-\alpha)|\lambda(s) - \lambda(s_0)|^2 - (s - s_0)^2 = 0 \tag{27}$$

When the Euler-Newton technique is applied to problem (24), computational difficulties near singularities are eliminated, since the Jacobian matrix P_x remains nonsingular near such points.

The above techniques, discussed in greater detail elsewhere (Keller, 1977; Heinemann et al., 1979) enabled us to locate broad regions of multiplicity for the rich hydrogen flame. Results of the computations are presented in the next section.

THE EFFECT OF THE HYDROPEROXYL AND SIMPLE MECHANISMS ON MULTIPLICITY

In this section and in the next, we show how the results of our calculations are affected by our choice of chemical mechanism. Multiple solutions for both mechanisms are shown in Figure 1, in which we plot the outlet temperature of the flame as a function of the burner surface temperature. The S shaped curve shown to the right of the figure represents the numerical solutions of the mathematical model using the hydroperoxyl mechanism, while the other curve represents solutions for the simpler, two-step mechanism. In each case, the lower solutions represent stable extinguished steady states, the intermediate solutions are unstable and the upper solutions represent stable burning states. The upper solutions may be divided into two classes. We shall later show that the flames represented by the long, horizontal section of the solution branch are nonadiabatic, while the shorter, sloping portion represents adiabatic flames.

The figure illustrates the sensitivity of flame multiplicity to chemical mechanism. The predictions of the thermal ignition temperature are greatly different for the two models. The model using the hydroperoxyl mechanism predicts an ignition temperature of 860°K, while the model using the simple scheme predicts ignition at 580°K.* Lewis and von Elbe (1961) reported a thermal ignition temperature of 820°K for a stoichiometric mixture of hydrogen and air at atmospheric pressure. Based on the prediction of ignition, the hydroperoxyl mechanism gives a much better kinetic description of the rich hydrogen flame.

Figure 1 also indicates significant differences in the prediction of burnout. The hydroperoxyl flame extinguishes at a burner surface temperature of 338°K and a maximum temperature of 1 045°K, while the simpler flame quenches at a burner temperature of 305°K and an outlet temperature of 950°K. The effect of the mechanisms on burnout and ignition will be discussed below.

In Figures 2 through 4 we present the oxygen, hydrogen and temperature profiles of the hydroperoxyl and simple flames for burner surface temperatures of 400°, 360° and 350°K, while Figure 5 shows the profiles at the predicted burnout conditions. This series of figures illustrates the transition from a well-stabilized, nonadiabatic flame to one which is metastable at burnout.

An examination of Figure 2, a nonadiabatic flame with a 400°K inlet temperature, reveals several qualitative distinctions between the two rival mechanisms. The sharp rise in the temperature profiles near the burner surface indicates that the flame is losing heat to the burner. Although the predicted profiles are quite similar, temperatures in the hydroperoxyl flame are

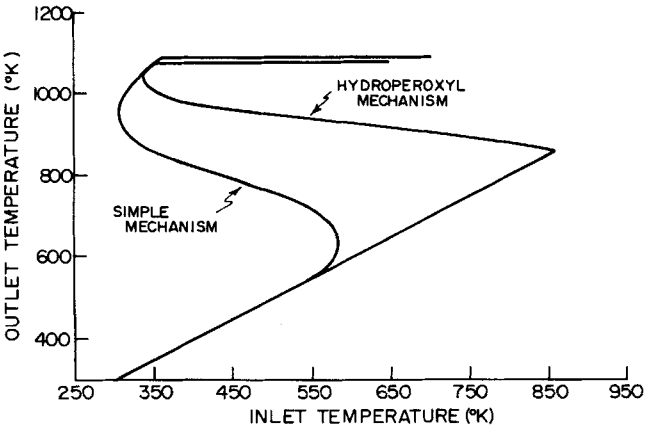

Figure 1. Multiple steady states of the rich hydrogen-oxygen-nitrogen flame for hydroperoxyl and simple kinetic mechanisms.

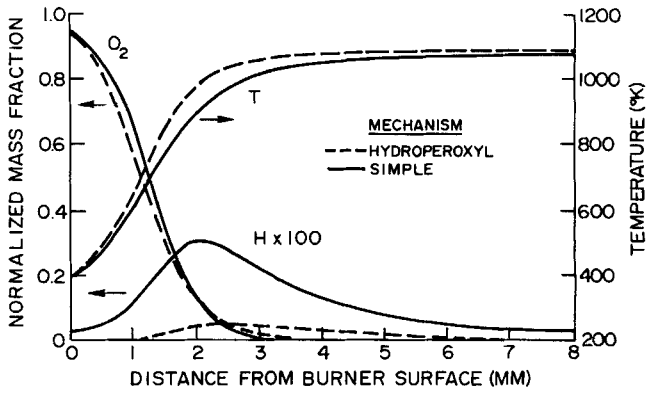

Figure 2. Temperature and concentration profiles of the hydroperoxyl and simple flames for an inlet temperature of 400°K.

somewhat larger. The oxygen profiles are similar, in both cases dropping rapidly near the inlet. Significant differences can be seen in the hydrogen profiles. The maximum hydrogen mole fraction in the hydroperoxyl flame is 0.00078 (at 1 040°K), and the maximum is 0.0048 (at 936°K) in the simple flame.* The smaller, more realistic, radical concentrations predicted by the hydroperoxyl model provide additional evidence for selecting this mechanism to describe the kinetics of rich hydrogen flames.

A comparison of the details of the two kinetic mechanisms explains the large hydrogen concentrations predicted by the two-step scheme. Both the simple and hydroperoxyl mechanisms produce radicals by reaction (ii-*a*). This initiation step has a comparatively small heat of reaction, so that nearly all of the energy generated in the flame must be supplied by reactions which consume hydrogen. In the simple mechanism, reaction (vii)—the only radical consumption step—releases about 90% of the heat in this flame. Since the reaction rate of (vii) is proportional to the square of the concentration of hydrogen atoms, the radical concentration must be quite high in order to release enough energy to support the temperature profile shown in Figure 2. The hydroperoxyl mechanism, on the other hand, contains two additional radical consumption steps, (iv-*a*) and (iv-*b*). These steps are highly exothermic, have higher reaction rates than (vii) and thus make it possible for the hydroperoxyl flame to maintain much lower hydrogen concentrations.

Figure 3 presents the composition and temperature profiles of a flat flame with an inlet temperature of 360°K. The features of these profiles are similar to those shown in Figure 2. This nonadiabatic flame reaches the same outlet temperature but

* We might note that the sharp turns in the multiplicity curves are not artifacts of the numerical method. A figure with an enlarged ordinate scale would show the S shaped curves to be rounded and smooth at the turning points.

* Dixon-Lewis (1970) has modeled an adiabatic, one-dimensional flame propagating through a gas mixture with the same concentrations and physical constants as the flames shown in Figures 2 through 5. For an adiabatic flame with a cold boundary temperature of 336°K, he reported a maximum hydrogen fraction of 0.001 occurring at 1 030°K in the hydroperoxyl flame and a maximum of 0.0053 in simple flame at 900°K.

loses less heat to the burner than the flame with an inlet temperature of 400°K. Temperature and composition profiles are less steep near the burner surface. The oxygen concentration at the surface is closer to its feed concentration, and the hydrogen profile is shifted further downstream from the burner.

A flame stabilized on a flat flame burner with a surface temperature of 350°K is shown in Figure 4. At this inlet temperature, the mathematical models predict significantly different flames. The model using the two-step mechanism again predicts a nonadiabatic flame, while the hydroperoxyl flame is now adiabatic. The temperature and composition profiles of the adiabatic flame are flat at the burner surface. This result and the additional observation that the normalized hydrogen and oxygen mass fractions equal zero and unity at the flame inlet are consistent with the boundary condition shown in Equation (19).

The role of the hot boundary conditions (20) in our computations deserves some attention, since it might be suggested that replacement of a boundary condition at infinity by one at $s = 1$, that is, at some finite flame thickness $(\psi_H - \psi_C)$, might influence the solution. In practice, increasing $(\psi_H - \psi_C)$ beyond the value shown in Table 2 extends the flat portion of the profiles (downstream of the reaction zone) without otherwise affecting the nature of the solution, while a decrease in $(\psi_H - \psi_C)$ simply leads to a failure to achieve zero derivatives at the hot boundary.

The results shown in Figure 4 are quite important because they illustrate the relative ease of discriminating between two rival mechanisms by comparing theoretical and experimental concentration and temperature profiles under optimal conditions. An examination of the profiles 3 mm above the burner surface reveals that the temperature predictions differ by 400°K, and the oxygen mass fractions differ by 0.70. The hydroperoxyl model predicts no atomic hydrogen at this position, while the simple flame model exhibits maximum hydrogen concentration at this point. Measurements of concentration and temperature profiles of a rich hydrogen flame at the conditions of Figure 4 would be extremely useful in elucidating kinetic mechanism.

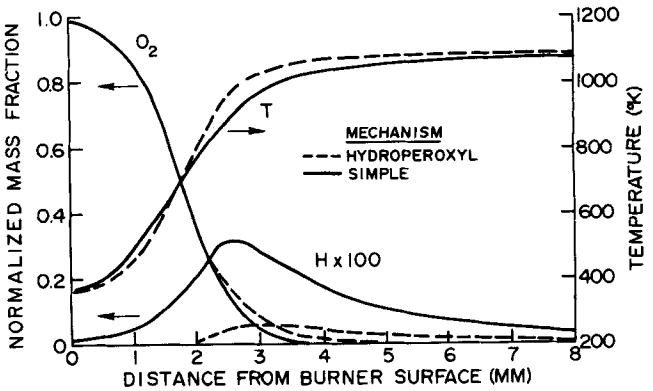

Figure 3. Temperature and concentration profiles of the hydroperoxyl and simple flames for an inlet temperature of 360°K.

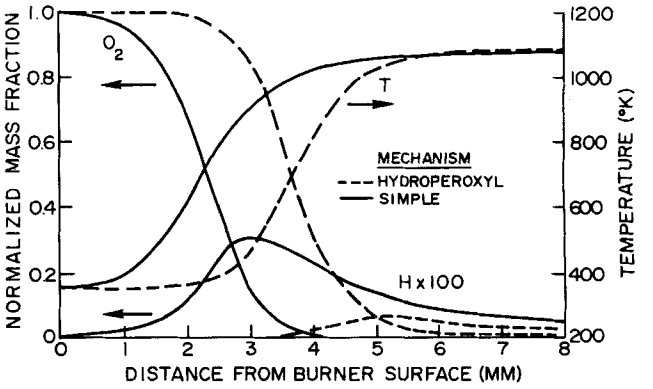

Figure 4. Temperature and concentration profiles of the hydroperoxyl and simple flames for an inlet temperature of 350°K.

ADIABATICITY, BURNOUT AND IGNITION

Both the hydroperoxyl and simple flames become adiabatic and approach burnout as the burner surface temperature is lowered below 345°K. The outlet temperatures fall, and the reaction zone moves away from the burner. Figure 5 presents concentration and temperature profiles at the predicted burnout conditions, and from these results we can identify the phenomena which characterize the quenching of the flame. At burnout, the distance between the burner surface and the reaction zone is greater than for any other stable flame. The reaction rates are slow, and the flame can just propagate back towards the burner at the rate at which reactants are supplied. The peak in the hydrogen radical profile is found at the flame outlet, and the maximum concentration of this chemically unstable species attains its largest value.

Although it can be no surprise that stability is enhanced by increasing heat transfer from flame to burner, it may at first seem paradoxical that the increased heat transfer is to be achieved by raising the burner temperature. The paradox can be resolved by reference to the kinetic mechanisms. The rate of reaction (ii-*a*) is relatively sensitive to temperature (see Table 1). As the burner surface temperature is lowered below 345°K, the rate of (ii-*a*) significantly decreases. This decrease retards radical production rate and therefore also slows reactions (iv-*a*), (iv-*b*) and (vii). [The reaction rates of (iv-*a*), (iv-*b*) and (vii) are proportional to the hydrogen concentration and are relatively insensitive to temperature.] When the burner temperature is lowered just below the quench point, the reaction rates are so slow that the reactants arriving from the burner cannot be consumed, and the flame is lifted off the burner.

The large difference in the predicted ignition points shown in Figure 1 can be attributed to the hydroperoxyl pathways included in the more complete mechanism. Along the lower portion of the hydroperoxyl solution branch, any hydrogen radicals produced by reaction (ii-*a*) are consumed by (iv-*b*) until the burner temperature is raised to within ½ deg of the thermal ignition temperature. At the ignition point, the radical production rate becomes sufficiently greater than the termination rate, and the thermal nature of the kinetic mechanism causes ignition. Hydrogen radicals produced by reaction (ii-*a*) are consumed in (iv-*b*) and (vii). The latter reactions produce heat, raise the temperature of the flame and increase the rate of (ii-*a*). This autothermal process is terminated by the depletion of oxygen, which limits the rate of (ii-*a*).

In the simple flame model, reactions (iv-*a*) and (iv-*b*) are absent, and only reaction (vii), which is very slow along the lower part of the solution branch, consumes radicals. Hence, hydrogen concentrations can build up at much lower burner temperatures and greatly reduce the ignition point.

THE EFFECT OF REACTION RATE COEFFICIENTS ON MULTIPLICITY

In this section we turn from a comparison of rival chemical mechanisms to a consideration of the effect of variations in a reaction rate coefficient within a single mechanism. We examine only one of the coefficients, Λ_7, the dimensionless reaction rate coefficient for the hydrogen ion recombination reaction, step (vii) in Table 1, and we consider only the hydroperoxyl mechanism. Effects of variations in all of the coefficients for both mechanisms are explored in detail by Heinemann (1979).

Figure 6 shows how the solution branch responds to a change in Λ_7.* Increasing Λ_7 accelerates step (vii), a highly exothermic reaction. As one might expect, such a change causes the nonadiabatic flames represented by the flat portions of the solution branches to burn at higher temperatures. This does not mean, however, that increasing the reaction rate coefficient of

* We remind the reader that $\Lambda_7 T_C^2$ is independent of T_C.

(vii) allows flames to survive at lower burner temperatures. Indeed, we see in Figure 6 that the flame with the lower value of Λ_7 remains stable at a lower inlet temperature.

We hypothesize an explanation by considering the effect of step (vii) on the hydrogen radical concentration and thus on the overall exothermicity and reaction rate. Consider a stable, nonadiabatic flame burning at a temperature of 400°K. At this inlet temperature, the effect of an increase in Λ_7 seems straightforward, exothermic reaction (vii) is accelerated and the outlet temperature increases. Now consider what happens as we lower the burner temperature, moving horizontally to the left in Figure 6. Lowering the inlet temperature has no effect on Λ_7, since it is independent of temperature (see Table 1). However, this decrease does retard radical generation step (ii), which is highly sensitive to temperature. As the temperature is lowered, the flame with the higher Λ_7 approaches adiabaticity and burnout first, since lower radical concentrations associated with larger Λ_7 coupled with the sensitivity of step (ii) to temperature greatly decrease the overall reaction rate, shifting the reaction zone away from the burner at higher inlet temperatures.

The ignition temperature is insensitive to Λ_7. This may be explained by noting that the hydroperoxyl pathways, rather than step (vii), control ignition, since they are highly exothermic, consume radicals and are much faster than (vii). [The rates of (iv-*a*) and (iv-*b*) are proportional to $\omega_{O2}\omega_H$, while the rate of (vii) is proportional to $(\omega_H)^2$; ω_H is extremely small near ignition.] We might also note that in the simple, two-step flame in which the hydroperoxyl pathways are absent, ignition temperature is quite sensitive to Λ_7 (Heinemann, 1979).

Figures 7 through 9 illustrate the effect of Λ_7 on the temperature and concentration profiles. The profiles are presented in Figure 7 for the hydroperoxyl flame at an inlet temperature of 400°K. The larger value of Λ_7 is suggested for the two-step mechanism. As expected from Figure 6, both flames are nonadiabatic, as evidenced by the steep slopes in the profiles at the burner surface. Also, the larger hydrogen concentrations as predicted using the smaller value of Λ_7 are consistent with previously stated hypotheses.

Figure 8 shows the profiles for an inlet temperature of 350°K. For this condition, we see the large differences in the predicted profiles of an adiabatic and nonadiabatic flame. A simple experiment which measured only the temperature profile of the flame would be extremely useful. At 2 mm above the burner surface, the predicted temperatures differ by 600°K.

It is, of course, generally accepted that flames are stabilized by losing heat to the burner, and our results confirm this idea. Figures 7 and 8 (also 2 through 4) indicate that flames with high inlet temperatures are quite nonadiabatic, highly stable and located close to the burner. Interestingly, as the inlet temperature is lowered, the flames lose less heat, are shifted away from the burner surface and approach burnout. As mentioned above, this transition is explained by the decreased overall reaction rates at lower temperatures.

Figure 9 presents the burnout profiles of the hydroperoxyl flame. Again, we see that at burnout the flame is just stabilized on the burner, the reaction zone is shifted from the surface and the radical concentration is maximized at the flame outlet. As previously discussed, the model using the smaller value of Λ_7 predicts larger hydrogen concentrations and lower burnout temperature. We point out that the temperature and concentration profiles for the flames in Figure 9 are quite similar, even though each flame has a different inlet temperature.

CONCLUSIONS

We have shown that near transitions between steady states, predicted behavior of a reaction-diffusion system is particularly sensitive to assumptions regarding chemistry and kinetics. So, for the hydrogen-oxygen-nitrogen flame, at least, numerical descriptions of ignition and burnout are quite useful in testing chemical models, in elucidating the relative importance of various chemical pathways and in quantifying reaction rate

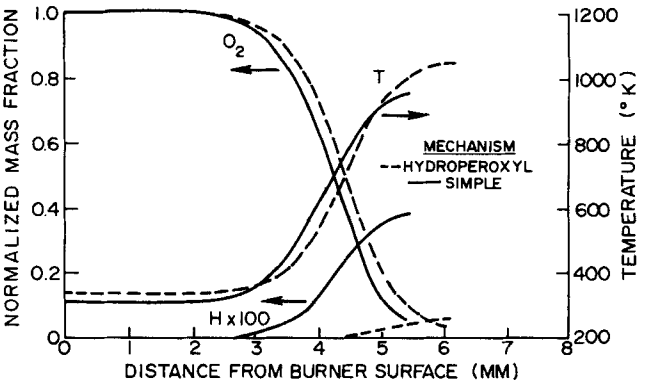

Figure 5. Temperature and concentration profiles of the hydroperoxyl and simple flames at burnout.

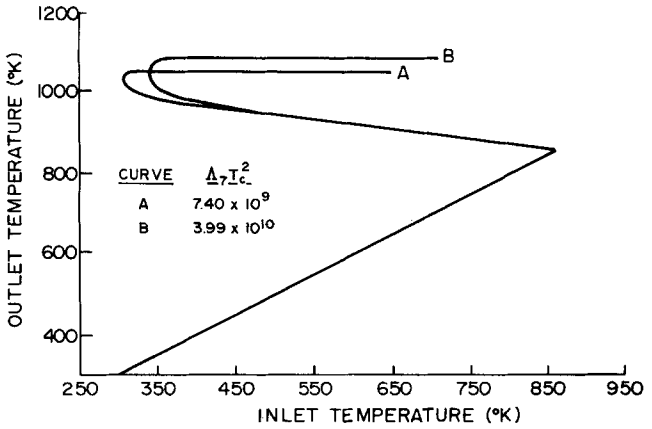

Figure 6. The effect of Λ_7 on the multiple solutions of the mathematical model of the rich hydrogen flame for the hydroperoxyl mechanism.

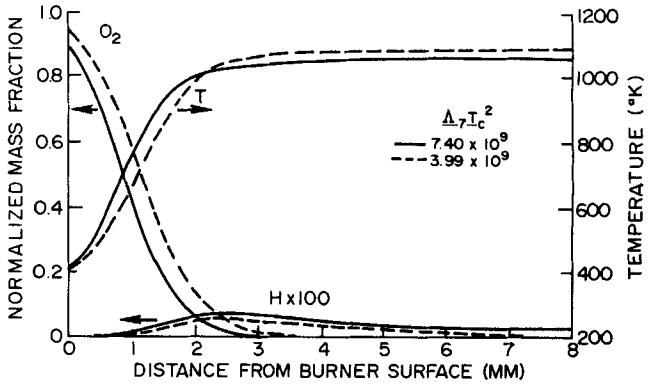

Figure 7. The effect of Λ_7 on the temperature and concentration profiles of the hydroperoxyl flame with an inlet temperature of 400°K.

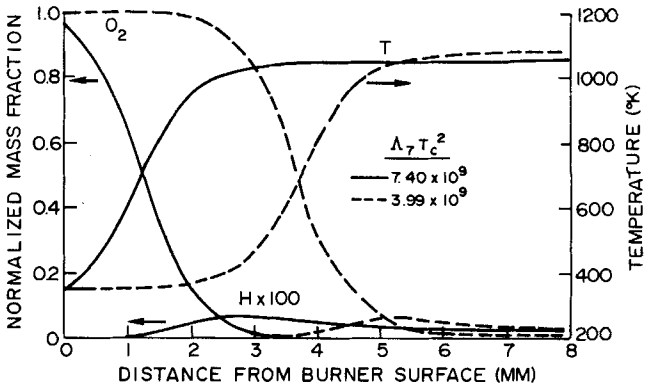

Figure 8. The effect of Λ_7 on the temperature and concentration profiles of the hydroperoxyl flame with an inlet temperature of 350°K.

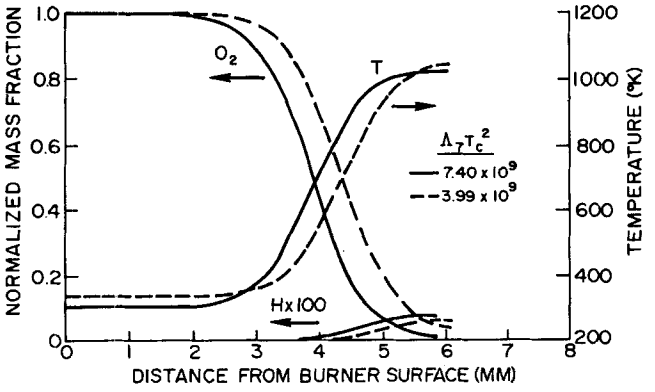

Figure 9. The effect of Λ_7 on the temperature and concentration profiles of the hydroperoxyl flame at burnout.

coefficients. It is to be hoped that analysis of such complex systems will eventually yield the sort of generalizable understanding that is now being developed in the study of simple reactions in the CSTR. Meanwhile, it is useful to note that numerical analytical techniques have been developed to such an extent that useful insight into chemical systems of industrial importance may be achieved through multiplicity analysis in those instances in which the rewards could be expected to justify the expense and difficulty involved.

NOTATION

A = frequency factor
C = concentration
C_p = specific heat
D = diffusion coefficient
ΔH = heat of reaction
k = thermal conductivity
k_i = reaction rate coefficient for reaction (i)
MW = molecular weight
Pe_O = Peclet number for mass transfer of oxygen
Pe_T = Peclet number for heat transfer
Pe_H = Peclet number for mass transfer of hydrogen
R = universal gas constant
R_1 = ratio of molecular weights of molecular oxygen and atomic hydrogen
R_2 = ratio of $\rho^2 D_{O_2}$ to $\rho^2 D_H$
s = dimensionless ψ coordinate
t = time
T = temperature
v = velocity
x = axial distance
y = normalized mass fraction of oxygen
z = normalized mass fraction of hydrogen

Greek Letters

γ = dimensionless activation energy
Λ = dimensionless frequency factor
θ = dimensionless temperature
ρ = density
ψ = transformation coordinate
ω = mass fraction

Subscripts

C = cold boundary of the flame
H = hot boundary of the flame
2 = reaction (ii-*a*)
7 = reaction (vii)
p = reaction (iv-*a*)
t = reaction (iv-*b*)

LITERATURE CITED

Berlad, A., "Thermokinetics and Combustion Phenomena in Nonflowing Gaseous Systems: An Invited Review," *Combust. Flame*, **21**, 275 (1973).

Bischoff, K. B., "A Note on Boundary Conditions for Flow Reactors," *Chem. Eng. Sci.*, **16**, 131 (1961).

Carrier, G. F., F. E. Fendell and W. B. Bush, "Stoichiometry and Flameholder Effects on a One-Dimensional Flame," *Combust. Sci. Technol.*, **18**, 33 (1978).

Chang, H., and J. M. Calo, "Exact Criteria for Uniqueness and Multiplicity of an nth Order Chemical Reaction via a Catastrophe Theory Approach," *Chem. Eng. Sci.*, **27**, 719 (1979).

Cohen, D. S., and A. B. Poore, "Tubular Chemical Reactors: The 'Lumping Approximation' and Bifurcation of Oscillatory States," *SIAM J. Appl. Math.*, **27**, 416 (1974).

Day, M. J., G. Dixon-Lewis and K. Thompson, "Flame Structure and Flame Reaction Kinetics VI—Structure, Mechanism and Properties of Rich Hydrogen + Nitrogen + Oxygen Flames," *Proc. Royal Soc. London*, **A330**, 199 (1972).

Dixon-Lewis, G., "Flame Structure and Flame Reaction Kinetics I. Solution of Conservation Equations and Application to Rich Hydrogen + Oxygen + Nitrogen Flames," *ibid.*, **A298**, 495 (1967).

———., "Flame Structure and Flame Reaction Kinetics V. Investigation of Reaction Mechanism in a Rich Hydrogen + Oxygen + Nitrogen Flame by Solution of Conservation Equations," *ibid.*, **A317**, 199 (1970).

———., and I. G. Shepard, "Some Aspects of Ignition by Localized Sources, and of Cylindrical and Spherical Flames" *Fifteenth Symposium (International) on Combustion*, p. 1483, The Combustion Institute, Pittsburgh, Pa. (1975).

Fang, M., R. A. Schmitz and R. G. Ladd, "Combustion of a Premixed System in Stagnation Flow—II. Experiments with Carbon Monoxide Oxidation," *Combust. Sci. Technol.*, **4**, 143 (1971).

Fristrom, R. M., and A. A. Westenberg, *Flame Structure*, McGraw-Hill, New York (1965).

Heinemann, R. F., K. A. Overholser and G. W. Reddien, "Multiplicity and Stability of Premixed, Laminar Flames: An Application of Bifurcation Theory," *Chem. Eng. Sci.*, **34**, 833 (1979).

———., "Multiplicity and Stability of Nonadiabatic Hydrogen-Oxygen-Nitrogen Flames," Ph.D. dissertation, Vanderbilt University, Nashville, Tenn. (1979).

Kanury, A. M., *Introduction to Combustion Phenomena*, Gordon and Breach, New York (1975).

Keller, H. B., "Bifurcation and Nonlinear Eigenvalue Problems," in *Applications of Bifurcation Theory*, P. H. Rabinowitz, ed., p. 359, Academic Press, New York (1977).

Kirkby, L. L., and R. A. Schmitz, "An Analytical Study of Diffusion Flame Stability," *Combust. Flame*, **10**, 205 (1966).

Lewis, B., and G. von Elbe, *Combustion, Flames and Explosions of Gases*, 2 ed., Academic Press, New York (1961).

Margolis, S. B., "Theoretical Analysis of Steady, Nonadiabatic, Premixed Laminar Flames," Sandia Lab. Rept. *SAND 78-8023* (1978).

Poore, A. B., "A Model Equation Arising From Chemical Reactor Theory," *Arch Rational Mech. Anal.*, **52**, 358 (1973).

Schmitz, R. A., "A Further Study of Diffusion Flame Stability," *Combust. Flame*, **11**, 49 (1967).

———., "Multiplicity, Stability and Sensitivity of States in Chemically Reacting Systems—A Review," *Adv. Chem. Ser.*, **148**, 156 (1975).

Smith, H. W., R. A. Schmitz and R. G. Ladd, "Combustion of Premixed System in Stagnation Flow—I. Theoretical," *Combust. Sci. Technol.*, **4**, 131 (1971).

Spalding, D. B., and P. L. Stephenson, "Laminar Flame Propagation in Hydrogen and Bromine Mixtures," *Proc. Royal Soc. London*, **A324**, 315 (1971).

Uppal, A., W. H. Ray and A. B. Poore, "On the Dynamic Behavior of Continuous Stirred Tank Reactors," *Chem. Eng. Sci.*, **29**, 967 (1974).

———., "The Classification of the Dynamic Behavior of Continuous Stirred Tank Reactors," *ibid.*, **31**, 205 (1976).

Varma, A., and N. R. Amundson, "Global Asymptotic Stability in Distributed Parameter Systems: Comparison Function Approach," *ibid.*, **27**, 907 (1972*a*).

———., "Some Observations Concerning the Nonadiabatic Tubular Reactor: A—Priori Bounds, Qualitative Behavior, Preliminary Uniqueness and Stability Considerations," *Can. J. Chem. Eng.*, **50**, 470 (1972*b*).

———., "Some Observations on Uniqueness and Multiplicity of Steady States in Nonadiabatic Chemically Reacting Systems," *ibid.*, **51**, 206 (1973*a*).

———., "The Nonadiabatic Tubular Reactor: Stability Considerations," *ibid.*, 459 (1973*b*).
Williams, F. A., "Theory of Combustion in Laminar Flows," *Ann. Rev. Fluid Mech.*, 3, 171 (1971).

Manuscript received August 2, 1979; and accepted January 23, 1980.

Chlorination Kinetics of Zirconia in an RF Chlorine Plasma Tail Flame

O. BICEROGLU
and
W. H. GAUVIN

Department of Chemical Engineering, McGill University
Montreal, Quebec, Canada

The chlorination kinetics of zirconia were studied in a single stationary particle reactor system. A plasma of pure chlorine generated by an induction torch provided both the high enthalpy field and the reacting gas. The influence on the rate of conversion of such parameters as temperature, chlorine concentration (in the presence of argon) and particle diameter and porosity were investigated. Based on experimental and theoretical studies, rate equations were developed under different rate controlling mechanisms.

The chlorination of zirconia in the particle temperature range of 1 540° to 2 480°K obeyed a shrinking core reaction model. The reaction was chemically controlled below 1 950°K, and above this temperature both chemical and mass transfer resistances were important. The experimental results confirmed the theoretical analysis.

SCOPE

The chlorination of zirconium oxide may be considered as an integral part of the overall process for the production of nuclear grade zirconium. The latter's commercial production is currently based on the Kroll process (Miller, 1954; Shelton et al., 1956; Starrat, 1959; Elger, 1962; Babu et al., 1969; Chintamani et al., 1972; Spink, 1977) which uses hafnium free, pure zirconium tetrachloride as the feed material. Newer processes which have been proposed to replace the conventional commercial method of production also use zirconium tetrachloride as the starting material. These include plasma decomposition of zirconium tetrachloride (Chizhikov, Deineka and Makarova, 1969; Chizhikov et al., 1971; Semenenko et al., 1975; Gragg, 1973; Little and Wentzell, 1965; CIBA, 1966) and electrowinning of the metal from fused salts containing zirconium tetrachloride (Martinez and Couch, 1972; Martinez et al., 1976).

For the production of nuclear grade zirconium, the near complete separation of hafnium, which is always associated with zirconium in the ore, is necessary owing to hafnium's high neutron absorption cross section. In the present conventional process, hafnium separation is effected by means of solvent extraction, to yield purified $Zr(OH)_4$. The latter is then calcined to yield dehafniated zirconia. The subsequent chlorination of the dioxide to produce the tetrachloride feed for the Kroll process is thus an essential processing step in the overall complex production scheme.

Zircon, the main source of the metal, may be either chlorinated directly (Manieh and Spink, 1973; Manieh, Scott and Spink, 1974) or through a two-step process, namely, the carburization of zircon followed by the chlorination of zirconium carbide or carbonitride (Kroll, Carmody and Schlechton, 1952; Stephens and Gilbert, 1952; Shelton et al., 1956). The former requires a larger reactor volume, extra chlorine and carbon for the silica constituent of the ore, for the same throughput of zirconium tetrachloride. Furthermore, it necessitates the separation, handling and disposal of silicon tetrachloride. On the other hand, the two-step process has been shown to be less efficient than zircon chlorination (Stephens and Gilbert, 1952). The recent development of a plasma process for the dissociation of zircon into its two constituent oxides zirconia and silica (Wilks et al., 1972, 1974; Bayliss, Bryant and Sayce, 1977) followed by leaching of the silica may lead in future to the direct chlorination of the impure zirconia thus produced rather than that of zircon.

The kinetics of the chlorination of zirconium oxide have not received much attention. The available publications in the field are limited to those of O'Reilly et al. (1972), Landsberg et al. (1972) for the kinetic study; to those of Stephen and Gilbert (1952) and Sehra (1974) for vertical shaft furnace and fluidized bed chlorination operation, respectively, and to that of Vasilenko and Volskii (1958) for thermodynamic analysis. All of these studies are concerned with temperatures below 1 400°K, under which conditions the reaction rates are too low for a viable industrial process.

In the present work, it was intended to study the kinetics of zirconium oxide chlorination at high temperatures (1 400° to 2 480°K). A chlorine induction plasma reactor system was used to provide both the high temperature field and the reactant gas. To the authors' knowledge, the generation of a plasma of pure chlorine has never been attempted before, nor has the use of a plasma system for chlorination kinetic studies.

To achieve the objectives of the study, a special reactor system had to be designed and developed to handle hot chlorine and control and measure all parameters affecting the rate of the heterogeneous zirconia chlorination. A theoretical analysis was carried out along with the experimental work.

O. Biceroglu is with Imperial Oil Ltd., Research Department, Sarnia, Ontario, Canada. W.H. Gauvin is with Noranda Research Centre, Pointe Claire, Quebec, Canada.

0001-1541-80-3899-0734-$01.15.